

Estimating Individual Cone Fundamentals from their Color Matching Functions

CASPER F. ANDERSEN^{1,*}, GRAHAM D. FINLAYSON², AND DAVID CONNAH³

¹Faculty of Computer Science and Media Technology, Norwegian University of Science and Technology, Gjøvik, 2802, Norway

²School of Computing Sciences, University of East Anglia, Norwich, NR4 7TJ, UK

³Centre for Visual Computing, University of Bradford, Bradford, BD7 1DP, UK

*Corresponding author: casper.andersen@ntnu.no

Compiled July 12, 2016

Estimation of individual spectral cone fundamentals from color matching functions is a classical and long-standing problem in color science. In this paper we propose a novel method to carry out this estimation based on a linear optimization technique, employing an assumption of a priori knowledge of the retinal absorptance functions. The result is an estimation of the combined lenticular and macular filtration for an individual, along with the nine coefficients in the linear combination that relates their color matching functions to their estimated spectral cone fundamentals. We test the method on the individual Stiles and Burch color matching functions and derive cone fundamental estimations for different viewing fields and matching experiment repetition. We obtain cone fundamental estimations that are remarkably similar to those available in literature. This suggests that the method yields results that are close to the true fundamentals. © 2016 Optical Society of America

OCIS codes: 330.5310, 330.1720

<http://dx.doi.org/10.1364/ao.XX.XXXXXX>

1. INTRODUCTION

The color matching functions (CMFs) form the basis of colorimetry and color specification. These functions describe the intensities of each of three primary lights that are required to match a test stimulus as a function of wavelength and they vary for different observers and different sets of primaries. The Commission Internationale d'Eclairage (CIE) has collected measured CMFs for a number of observers and averaged these across observers to derive a standardized set of CMFs [1]. These functions are used to specify the photopic color response of the standard observer to any color stimulus. The most common standard observer adopted by the CIE, the XYZ color matching functions, uses imaginary primaries to ensure that the resulting tristimulus values are always positive and the Y value is equal to the photopic luminous efficiency function. These are defined for stimuli subtending 2 degrees and 10 degrees at the retina [2] (the so-called 2-degree and 10-degree observers).

An alternative to XYZ tristimulus values for representing the spectral response of human vision is given by the quantal catches of the cones. Cone quantal catches provide better inputs for color vision models since they represent the actual amount of light absorbed in the eye and thus the true signal captured at the retina, whereas XYZ values are never represented explicitly within the human visual system [3]. The wavelength sensitivity

of a cone sensor is commonly equivalently expressed in terms of a spectral sensitivity function called a fundamental. In normal trichromatic vision there are three such fundamentals known as the LMS-functions. They are three different, linearly independent spectral functions, the longwave $l(\lambda)$, middlewave $m(\lambda)$ and shortwave $s(\lambda)$ functions. As their names indicate, each function has a maximum and predominant sensitivity in the long-, middle- or shortwave part of the visible spectrum. The cone fundamentals are also within a 3×3 linear transformation of the CMFs and as such are a set of CMFs themselves.

Unfortunately, the cone fundamentals do not correspond to a physically realisable or known set of primary lights. Accordingly, estimates of these fundamentals must be derived indirectly by firstly measuring a set of CMFs and then determining the parameters of the 3×3 transformation matrix. To estimate these parameters requires the incorporation of additional measurements and assumptions. This can involve measuring CMFs from additional color normal and color deficient observers, evaluating the genetic predisposition of observers, direct measurements in vitro or in situ of the cones [4, 5] and assumptions relating to the usage of measurements across different observers [2]. The most recent set of standard LMS functions that are in common use were derived by Stockman and Sharpe in [6].

While these standardized functions can be derived for an av-

erage observer, it is well known that individual differences, and thus deviations from the standard, exist. There can be many reasons for individual variation, including genetic polymorphism in spectral positioning of cone pigments for trichromats [7, 8], anomalous trichromacy (where there is large overlap between cone sensitivities), dichromacy (where cone types are missing), and optical density variations in the ocular media, macular pigment and retinal pigmentation [9]. The result of the above is that although CMFs can be estimated for individuals through a color matching experiment, the standard transformations to compute cone fundamentals are no longer valid since the assumptions employed do not hold for individuals.

Here, we present a novel method for estimating cone fundamentals from CMFs for individuals [12]. We assume that the main source of variation between individuals stems from differences in the absorption in the ocular media and the macular pigmentation (supported by the findings in [13]) which implies that the photo-pigment absorptances are known [14], and are constant across observers. This assumption leads us to an iterative method which simultaneously estimates ocular and macular absorption, which we combine into a single pre-filter, and which is used to relate the known absorptances to estimated cone fundamentals. We show that the method produces reliable and stable estimates of cone fundamentals across a range of individual observers.

2. BACKGROUND

Given a color with spectral power distribution $S(\lambda)$, the tristimulus values for that color can be computed using the color formation equations:

$$\begin{aligned} R &= k \int_{\omega} r(\lambda) S(\lambda) d\lambda \\ G &= k \int_{\omega} g(\lambda) S(\lambda) d\lambda \\ B &= k \int_{\omega} b(\lambda) S(\lambda) d\lambda \end{aligned} \quad (1)$$

where R , G , and B denote the tristimulus values, ω denotes the range of visible wavelengths λ , k is a constant, and $r(\lambda)$, $g(\lambda)$, and $b(\lambda)$ denote a set of color matching functions (CMFs).

Although altering the primary lights used to derive the CMFs necessarily changes them, these functions are always, through the Grassmann Laws ([2], p. 118) linearly related to one another by a 3×3 matrix multiplication. So, given two sets of color matching functions $\mathbf{CMF}_i(\lambda) = [r_i(\lambda) \ g_i(\lambda) \ b_i(\lambda)]$, $i \in [1, 2]$, derived from two sets of primaries, we have:

$$\mathbf{CMF}_1(\lambda) = \mathbf{CMF}_2(\lambda) \mathbf{M} \quad (2)$$

where \mathbf{M} denotes a 3×3 matrix.

An observer's spectral cone sensitivities $\mathbf{LMS}(\lambda)$ are a special set of color matching functions and are therefore linearly related to other sets of CMFs in the same way:

$$\mathbf{LMS}(\lambda) = \mathbf{CMF}(\lambda) \mathbf{M} \quad (3)$$

where:

$$\mathbf{LMS}(\lambda) = [l(\lambda) \ m(\lambda) \ s(\lambda)] \quad (4)$$

and the matrix \mathbf{M} takes the form:

$$\mathbf{M} = \begin{bmatrix} l(e_1) & m(e_1) & s(e_1) \\ l(e_2) & m(e_2) & s(e_2) \\ l(e_3) & m(e_3) & s(e_3) \end{bmatrix} \quad (5)$$

In these equations e_1, e_2, e_3 are the wavelengths of primaries corresponding to the color matching functions in $\mathbf{CMF}(\lambda)$ [2]. Equation 5 follows because the i th CMF for a given primary e_i has the property that $\mathbf{CMF}(e_i) = 1$, whereas the other two CMFs are exactly zero at e_i .

It is clear from the definition above that the coefficients of \mathbf{M} are given by the response of the $l(\lambda)$, $m(\lambda)$, and $s(\lambda)$ functions to the three primaries used to derive the CMFs. However, when the goal is to estimate the fundamentals these quantities are clearly unknown, and certain assumptions need to be employed to estimate them. It is worth noticing that \mathbf{M} equivalently could be expressed as an inverse of a matrix whose elements are the color matching functions $r(\lambda)$, $g(\lambda)$, and $b(\lambda)$ responses to the primaries of the fundamentals. But since they are unknown that will not immediately bring the solution closer.

The most common approach to solving for \mathbf{M} is to use the König assumption [2], which states that dichromatic (protanope, deuteranope or tritanope) vision is a reduced form of normal trichromatic vision defined by the lack of one of the three trichromatic cone sensors. Thus combining the CMFs of trichromatic vision with dichromat metamerism measured for the three types of dichromats, yields three confusion points in chromaticity space that uniquely define the linear transformation between the color matching functions and the cone fundamentals [6, 15–17].

The König assumption, and related constraints, can be applied to CMFs that have been derived by averaging CMFs across observers, but since CMFs measured for individuals can differ significantly from the standard this approach is not feasible for the estimation of individual fundamentals. A detailed investigation of the specific causes of variation in [13] found that the inter-observer variations in the Stiles-Burch 10 degree CMFs are sufficiently explained by differences in the lens- and the macular-pigment optical densities, in the degree of rod intrusion in the matches and in the optical peak densities and peak wavelengths of the individual photo pigments. There it is suggested that the variations in lens and the macula are sizeable contributors to the overall individual variations. Polymorphism and variations in photo-pigment optical density are also important, although the variations in peak-wavelengths seem to be smaller, or about the size of the sampling frequency of the color matching data (i.e. circa 5 nm).

As a consequence of these variations, although CMFs can be measured for individuals through a color matching experiment, the standard methods to derive cone fundamentals fail, since the assumptions employed cannot be applied for individuals. To estimate individual LMS functions from individual CMFs, different constraints must be imposed on the solution.

For any individual set of color matching functions, the problem we are addressing here is to find the 9 coefficients $m_{i,j}$ in \mathbf{M} that transform the color matching functions into the corresponding spectral cone fundamentals. The classic approach, devised by Bongard and Smirnov, works by the assumption that the fundamental functions, throughout the visible spectrum, only partly overlap each other, leaving wavelengths to be found in which one or two of the three functions are zero. They use this to define three particular sets of three primaries, for which each of the corresponding sets of color matching functions, within a scaling factor, must contain either one of the L, M or S functions.

Say e_1^* , e_2^* and e_3^* are the primaries of color matching functions $\mathbf{CMF}^*(\lambda) = [r^*(\lambda) \ g^*(\lambda) \ b^*(\lambda)]$. Then for example, for the

longwave fundamental $l(\lambda)$ in Equation 3:

$$l(\lambda) = l(e_1^*)r^*(\lambda) + l(e_2^*)g^*(\lambda) + l(e_3^*)b^*(\lambda) \quad (6)$$

when using Equation 4 and Equation 5 wherein primaries e_1^* , e_2^* and e_3^* are inserted. Exploring the reduced overlap assumption, then the primaries e_2^* and e_3^* can be chosen in the short wavelength interval making sure that $l(e_2^*) = l(e_3^*) = 0$ and e_3^* can be chosen in the long wavelength interval so that $l(e_1^*) \neq 0$. From Equation 6 it clearly follows that $l(\lambda) = l(e_1^*)r^*(\lambda)$ whereby the longwave fundamental, within an unknown scaling factor $l(e_1^*)$, is found as the long wave color matching function $r^*(\lambda)$. A second and a third set of primaries can likewise be defined to calculate the middlewave and shortwave fundamentals.

This approach has since been used by Speranskaya and Lobanova in order to study anomaly [18, 19] and revisited by Logvinenko [20] with the purpose of estimating individual cone sensitivities from color matching functions.

The Bongard and Smirnov method, however, has some reported shortcomings. The assumption that cone functions have zero response in certain wavelengths, e.g. that L and M cones have zero response at short wavelengths is only approximately true. This is particularly pronounced in the long-wave cone fundamental and it is related to a small rhodopsin based short-wavelength sensitivity known as the "cis"-peak [21–23]. Furthermore, had the pairwise overlap in the wavelength interval extremities been strictly true, then the spectrum locus would have consisted of two straight lines there. This is contrary to fact [1]. This, coupled with noise in the measurement of the CMFs, makes the method unstable, results in small negative lobes around the chosen primaries of the estimated cone functions and therefore gives rise to inaccurate estimates.

To avoid having to select certain wavelengths as primaries and thus get negative lobes around them and to stabilize the estimations, in [11] the authors devised a simple rank based method, which relies on the fact that the dimensionality of a set of functions (i.e. CMFs) is invariant to any full rank transformation. By applying singular value decomposition to the color matching functions in the full visual spectrum ω , five successive wavelength subintervals, δ_k where $k = 1, 2, \dots, 5$ are found that delimit the number of linearly independent overlapping fundamentals in the interval. The number of overlapping functions (or dimensions) in each of these intervals are, as a function of progressing wavelengths, 1 dimension in δ_1 , 2 in δ_2 , 3 in δ_3 , 2 in δ_4 and 1 in δ_5 .

To estimate the fundamentals a bounded and positivity constrained linear optimization is employed. Each i^{th} fundamental is found in subintervals ω_i for $i = 1, 2, 3$ in which it is thus known to have a non-zero response.

$$\omega_1 = \delta_3 \cup \delta_4 \cup \delta_5 \quad (7)$$

$$\omega_2 = \delta_2 \cup \delta_3 \cup \delta_4 \quad (8)$$

$$\omega_3 = \delta_1 \cup \delta_2 \cup \delta_3 \quad (9)$$

The areas A_i under the estimated cone fundamentals are maximized

$$A_i = \max_{m_{i,j}} \int_{\omega_i} \mathbf{CMF}(\lambda) [m_{i,1} \ m_{i,2} \ m_{i,3}]^T \quad (10)$$

where the color matching functions are normalized to unit area in the full spectrum:

$$\int_{\omega} \mathbf{CMF}(\lambda) d\lambda = [1 \ 1 \ 1]^T \quad (11)$$

and the matrix coefficients $m_{i,j}$ in \mathbf{M} from Equation 5 are bounded by:

$$\sum_{i=1}^3 m_{i,j} = 1 \quad (12)$$

and constrained by positivity:

$$l(\lambda), m(\lambda), s(\lambda) \geq 0 \quad (13)$$

Although this method improves on the robustness of Bongard and Smirnov's approach, problems with the long-wave cone fundamental still remain.

3. METHOD

A. Physical parameters

In order to understand better the mechanisms behind individual variations we extend the basic Equations to include more physical parameters in the definition of the cone fundamentals. Specifically, the cone fundamentals are related to the retinal photo-pigment spectral absorptance $\mathbf{PDT}(\lambda)$ by the lens- and macular optical density functions combined in one pre-filter function $F(\lambda)$ [25]:

$$\mathbf{LMS}(\lambda) = F(\lambda)\mathbf{PDT}(\lambda) \quad (14)$$

where:

$$\mathbf{PDT}(\lambda) = [p(\lambda) \ d(\lambda) \ t(\lambda)] \quad (15)$$

and $p(\lambda)$ is the long wave, $d(\lambda)$ is the middle wave and $t(\lambda)$ short wave photo-pigment spectral absorptance. The functions are shown in Figure 1.

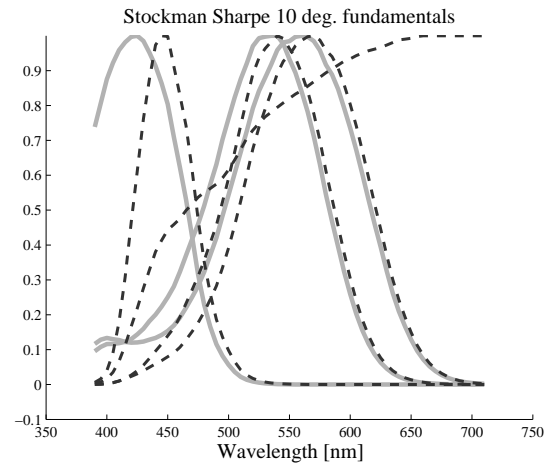


Fig. 1. Plot of the Stockman and Sharpe cone fundamentals (3 dashed gray curves) and the corresponding photo-pigment absorptances (3 full gray curves) and the combined ocular and macular pre-filter (monotonic dashed curve) as a function of wavelength. The functions are all normalized to unit peak value.

By definition [26], spectral absorptance $\alpha_{\lambda_p}^{\delta_p}(\lambda)$ pertaining to a specified peak wavelength λ_p and peak optical density δ_p expressed in terms of energy units is:

$$\alpha_{\lambda_p}^{\delta_p}(\lambda) = (1 - 10^{-\delta_p A_{\lambda_p}(\lambda)}) \lambda \quad (16)$$

where $A_{\lambda_p}(\lambda)$ is the spectral absorptance (also known as optical density) pertaining to a nominal peak optical density $A_{\lambda_p}(\lambda_p) =$

1. The spectral absorbance can be either tabulated [6, 27] (which we are using here) or formulated in templates of polynomial or exponential functions of wavelength [6, 28, 29]. Assuming a known absorbance function in Equation 16 can model a specific set of absorbance functions. This is used in [30] to develop an individual colorimetric observer.

The peak optical density varies over the surface of the retina as the thickness of the pigment layer varies. Toward the center of the retina (foveola) the pigment layer thickens as the concentration of cones increases and thus the optical density becomes larger. This means that there is an important difference between the absorbance spectra of foveal and parafoveal vision. This difference is one of the reasons for the partition of standard observers into small field 2 degree and large field 10 degree observers. The absorbance spectra broadens and the peak stays largely the same as δ_p increases. (The peak geometrically stays the same if the absorbance functions are measured in quantal units by omitting the multiplication with λ).

A complete mathematical relationship between CMFs and spectral absorbance comes from inserting Equation 14 into Equation 3, and dividing by $F(\lambda)$ for convenience, which yields:

$$F(\lambda)^{-1} \mathbf{CMF}(\lambda) \mathbf{M} = \mathbf{PDT}(\lambda) \quad (17)$$

The objective of our method, set forth in the remainder of this Section, is to simultaneously estimate the individual pre-filter $F(\lambda)$ and the individual matrix \mathbf{M} , based on the assumption that the photo-pigment absorbances $\mathbf{PDT}(\lambda)$ are known and in common for each of the individual color matching functions.

B. Discretizing the problem

In practice the color matching functions and absorbance functions are not represented explicitly as continuous functions as in Equation 17, but rather are represented as measurements made at discrete wavelengths, thus forming vectors of observations. As a result all optimisations presented here are formulated as discrete, matrix-vector, equations. Equation 17 therefore becomes:

$$\mathbf{D} \mathbf{W}_{cmf} \mathbf{M} = \mathbf{W}_{pdt} \quad (18)$$

where \mathbf{D} is an $N \times N$ diagonal matrix with the inverse pre-filter function $F(\lambda)^{-1}$, sampled at N equally spaced discrete wavelengths across the visible spectrum, along the leading diagonal. Similarly, \mathbf{W}_{cmf} is an $N \times 3$ matrix of discretely sampled color matching functions and \mathbf{M} is still a 3×3 matrix.

C. Unconstrained method

Solving for \mathbf{D} and \mathbf{M} is carried out by firstly rearranging Equation 18 to define a linear least squares minimization problem:

$$\min_{\mathbf{D}, \mathbf{M}} \|\mathbf{D} \mathbf{W}_{cmf} \mathbf{M} - \mathbf{W}_{pdt}\|^2 \quad (19)$$

In order to solve this, we employ an iterative scheme with two sets of coupled equations. Firstly, at iteration level k , we define N equations as a linear least squares minimization and solve for \mathbf{D}^{k+1} :

$$\min_{\mathbf{D}^{k+1}} \|\mathbf{D}^{k+1} \mathbf{W}_{cmf} \mathbf{M}^k - \mathbf{W}_{pdt}\|^2 \quad (20)$$

Secondly, we define a set of 3 equations as a linear least squares minimization and solve for \mathbf{M}^{k+1} :

$$\min_{\mathbf{M}^{k+1}} \|\mathbf{D}^{k+1} \mathbf{W}_{cmf} \mathbf{M}^{k+1} - \mathbf{W}_{pdt}\|^2 \quad (21)$$

\mathbf{D}^{k+1} and \mathbf{M}^{k+1} are solved for using closed form linear least squares [32]. As formulated, the estimate of \mathbf{D} and \mathbf{M} is found

iteratively solving for \mathbf{D} then \mathbf{M} . This alternating least-squares procedure converges. We simply stop the iteration when the estimates found at step $k+1$ are the same as those found in step k (practically, the estimates change less than a criterion amount epsilon). The final solution for the estimated cone fundamentals \mathbf{LMS}^{est} are calculated by either:

$$\mathbf{W}_{lms}^{est} = \mathbf{W}_{cmf} \mathbf{M}^k \quad (22)$$

or

$$\mathbf{W}_{lms}^{est} = (\mathbf{D}^k)^{-1} \mathbf{W}_{pdt} \quad (23)$$

The uniqueness of this solution is demonstrated in Section E.

In Figure 2 we show the recovered cone fundamentals and pre-filters found using the unconstrained method. While the recovered cones appear plausible the pre-filtering has 'jitter' (high frequency terms) whereas we would expect a very smooth (probably monotonic) functions.

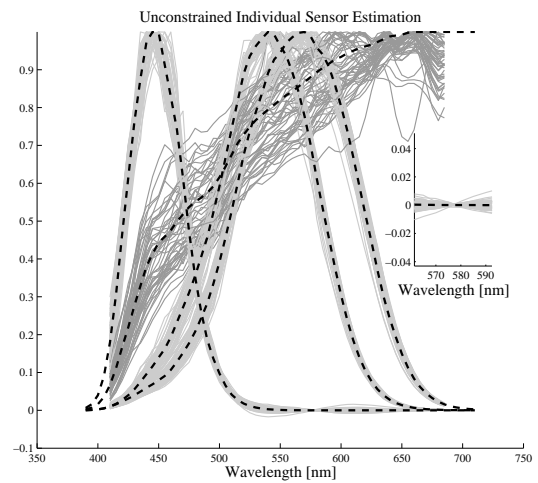


Fig. 2. Sensor estimation based on individual Stiles-Burch 10 deg. (1959) color matching functions. The unconstrained iterative method is used. Estimated fundamentals (light gray full curves), Estimated pre-filters (dark gray full curves), Stockman and Sharpe cone fundamentals (black broken curves) and pre-filter (black broken curves). Inset, S-cone estimates negative lobes.

D. Constrained method

In order to combat jitter we impose the constraint that the pre-filtering function is monotonically increasing. Specifically, we incorporate a constraint of non-negative first derivative of the estimated pre-filter function $F(\lambda)$:

$$F(\lambda_{i+1}) - F(\lambda_i) \geq 0 \quad (24)$$

To solve for the pre-filter \mathbf{D} - a least squares quadratic objective function - subject to this new linear constraint we use quadratic programming. Quadratic programming is a general framework for finding the unique global minimum for quadratic objectives subject to linear constraints.

While the recovered cone fundamentals look reasonable we see in Figure 2 in the inset, that there are small negative sensitivities. This is obviously impossible and we need to add a

second, positivity, constraint to mitigate this problem. We add the following constraint:

$$(\mathbf{D}^k \mathbf{W}_{cmf}) \mathbf{M}^k \geq 0 \quad (25)$$

Again subject to this constraint we can find \mathbf{M}^k using quadratic programming.

E. Uniqueness of solution

In [37] the uniqueness of the linear relation between an individual set of color matching functions and a corresponding set of cone fundamentals is questioned. Analyzing the observer metamerism between individuals from the Stiles and Burch dataset, using spectral stimuli from the object color solid (i.e. reflecting surfaces), the authors found that the metamerism is minimal between observers whose cone fundamentals differ by symmetrically shifted peak wavelengths (either away from or toward each other) of the middle and long-wavelength cone fundamentals. This observation brings doubt to the viability of estimating the cone fundamentals from an individual set of color matching functions since minimal observer metamerism between two observers means that their color matching functions are linearly related. It follows from this that two different sets of cone fundamentals would yield the same color matching functions.

In our method, however, we incorporate the assumption that the absorptions are fixed. This results in a unique relation between fundamentals and color matching functions, which we show below.

We demonstrate the uniqueness of our argument by contradiction. Suppose two different solutions to equation 18 exist for the matrix \mathbf{M}_1 and \mathbf{M}_2 and the pre-filter \mathbf{D}_1 and \mathbf{D}_2 along with two different absorptances $\mathbf{W}_{pdt,1}$ and $\mathbf{W}_{pdt,2}$ that are linearly related by:

$$\mathbf{W}_{pdt,1} \mathbf{N} = \mathbf{W}_{pdt,2} \quad (26)$$

where \mathbf{N} is a 3×3 matrix, then:

$$\mathbf{D}_1 \mathbf{W}_{cmf} \mathbf{M}_1 = \mathbf{W}_{pdt,1} \quad (27)$$

and

$$\mathbf{D}_2 \mathbf{W}_{cmf} \mathbf{M}_2 = \mathbf{W}_{pdt,2} \quad (28)$$

Combining Equations 27 and 28 using Equation 26 gives:

$$\mathbf{D}_1 \mathbf{W}_{cmf} \mathbf{M}_1 \mathbf{N} = \mathbf{D}_2 \mathbf{W}_{cmf} \mathbf{M}_2 \quad (29)$$

which leads to:

$$\mathbf{W}_{cmf} \mathbf{M}_1 \mathbf{N} \mathbf{M}_2^{-1} = \mathbf{D}_1^{-1} \mathbf{D}_2 \mathbf{W}_{cmf} \quad (30)$$

If we for clarity redefine $\mathbf{A} = \mathbf{M}_1 \mathbf{N} \mathbf{M}_2^{-1}$, $\mathbf{\Lambda} = \mathbf{D}_1^{-1} \mathbf{D}_2$ and $\mathbf{X} = \mathbf{W}_{cmf}$ then Equation 30 becomes:

$$\mathbf{X} \mathbf{A} = \mathbf{\Lambda} \mathbf{X} \quad (31)$$

in which case $\mathbf{\Lambda}$ must contain eigenvalues and \mathbf{X} must contain the corresponding eigenvectors of the transformation in the square matrix \mathbf{A} . However, \mathbf{A} is a 3×3 matrix so at most 3 eigenvector and eigenvalue pairs exist for \mathbf{A} , whereas Equation 31 implies that N independent pairs of eigenvectors and eigenvalues exist. Since that can not be the case, it follows that only one unique solution exists to Equation 18.

4. RESULTS

We apply our method to two sets of classical individual color matching function data sets provided by the work of Stiles and Burch [34, 35]: the 2 degree Color Matching Functions (1955) [36] and the 10 degree Color Matching Functions (1959). Measured CMFs are plotted in Figures 3 and 4.

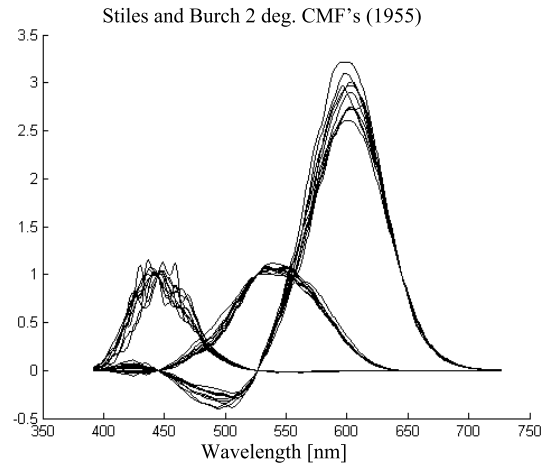


Fig. 3. Plot of the Stiles-Burch 2 degree 1959 color matching functions as a function of wavelength. The functions are all normalized to unity at the locations of the primaries.

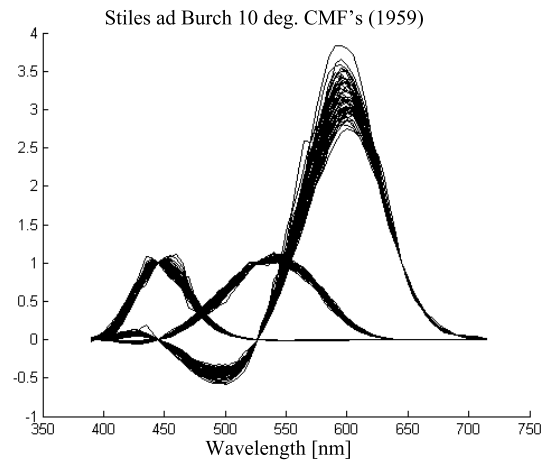


Fig. 4. Plot showing the Stiles-Burch 10 degree 1959 color matching functions as a function of wavelength from which 51 have been chosen. The functions are all normalized to unity at the locations of the primaries.

As an approximation to the photo-pigment absorptances $p(\lambda)$, $d(\lambda)$, $t(\lambda)$ used in the present investigation we use the Stockman-Sharpe absorbance function template [6], their peak optical wavelengths of 420.7, 530.3 and 558.9 nm for the short, medium and long wavelength pigment respectively and their peak optical densities [33] (see Table 1) regarding their 2 and 10 degree cone fundamental estimations.

The spectral absorptances $A_{558.3}(\lambda)$, $A_{530.3}(\lambda)$ and $A_{420.7}(\lambda)$ for each of the three photo-pigments are tabulated in [27] (in normalized logarithmic quantal units on a wavelength basis) and shown in Figure 5.

Inserting these spectral absorbance functions and the appropriate optical densities in Equation 16 yields spectral absorbance functions for each of the three cones pertaining to peak wavelengths of 420.7, 530.3 and 558.9 nm for the short, medium and long wavelength pigment respectively. For the 2 degree viewing field:

$$p_2(\lambda) = \alpha_{558.9}^{0.50}(\lambda), d_2(\lambda) = \alpha_{530.3}^{0.50}(\lambda), t_2(\lambda) = \alpha_{420.7}^{0.40}(\lambda) \quad (32)$$

and for the 10 degree viewing field:

$$p_{10}(\lambda) = \alpha_{558.9}^{0.38}(\lambda), d_{10}(\lambda) = \alpha_{530.3}^{0.38}(\lambda), t_{10}(\lambda) = \alpha_{420.7}^{0.30}(\lambda) \quad (33)$$

The 10 degree fundamentals are shown in Figure 1. Note that between 615 and 830 nm the short-wavelength absorbance function $t(\lambda)$ is taken to be zero (i.e. the left full gray curve in the figure).

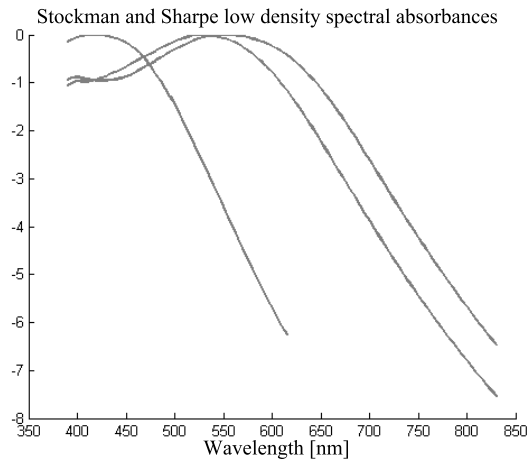


Fig. 5. Plot of the Stockman Sharpe low density spectral absorbances $A_{558.9}(\lambda)$, $A_{530.3}(\lambda)$ and $A_{420.7}(\lambda)$ for each of the three photo-pigments.

Table 1. Stockman and Sharpe, Peak Photo-pigment Optical Densities for the 2 and 10 degree Cone Fundamentals [33]

Observer	D^p	D^d	D^t
2 deg.	0.50	0.50	0.40
10 deg.	0.38	0.38	0.30

We have applied our method to the Stiles-Burch 10 degree 1959 slit width corrected color matching function data. Of the 53 data sets of color matching functions we have used 51, since two sets do not contain complete data. The data is given on a wavenumber basis (in intervals of 500 cm^{-1} from 25500 to 1400 cm^{-1}) and thus needs re-interpolation on a wavelength basis. We have done this using a standard third order polynomial piece-wise spline function, and the fact that the relation between λ (wavelength in nm) and wavenumber wn is given by:

$$\lambda = 10^7 / wn \quad (34)$$

The wavelength interval chosen, between 395 and 710 nm, is 5 nm which is approximately the interval which polymorphic

variation (variation in absorbances peak wavelength value) covers and at the same time is marginally smaller than the smallest interval in wavenumber (approximately 8 nm).

A. Consistency check

Firstly, to check the consistency of the method, we applied the constrained iterative method to the Stockman and Sharpe 10 degree Color Matching Functions using the corresponding Stockman and Sharpe 10 degree absorbance functions as constraints. In this test we are guaranteed that there is no error in Equation 18 and hence our method should produce the exact 10 degree fundamentals. The result is shown in Figure 6 with the Stockman and Sharpe cone fundamentals (black broken curves) and pre-filter (black broken curve) plotted alongside the estimated cone fundamentals (light gray unbroken curve) and pre-filter (dark gray unbroken curve). As expected, the real and the estimated functions coincide perfectly.

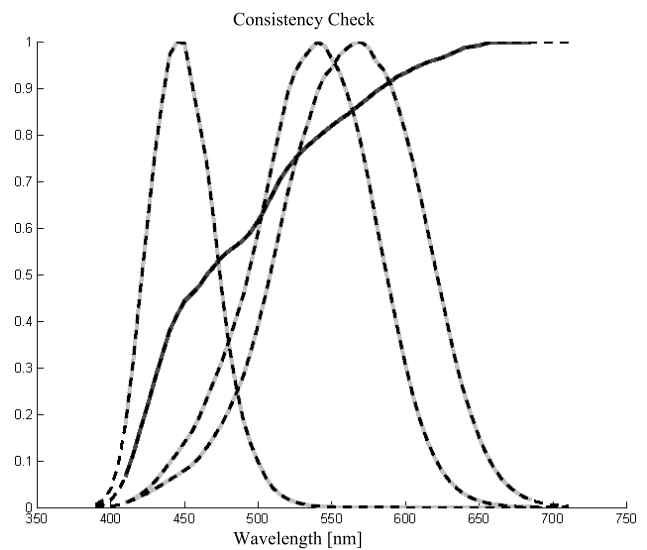


Fig. 6. Method consistency check: The tabulated (CVRL database) 10 degree cone fundamentals of Stockman and Sharpe Sensor (black broken curves) and pre-filter (black broken curve) plotted with the estimated cone fundamentals in light gray full curves and pre-filter dark gray full curve. Results based on the constrained iterative method.

B. Application of the method to 10 deg. Stiles and Burch Data

Secondly, we applied the method to CIE1964 10 degree Standard Observer Color Matching Functions, which are predominantly (thus not entirely) derived from the Stiles and Burch 10 degree color matching functions. The result is shown in Figure 7, where the Stockman and Sharpe 10 degree cone fundamentals (black broken curves) and the corresponding pre-filter (black broken curve) are plotted with the estimated cone fundamentals (light gray full curves) and their corresponding estimated pre-filters (dark gray full curve). The results again show a very close match in the cone fundamental estimation, with a small error in the pre-filter estimation.

C. Stiles and Burch Color Matching Functions

To demonstrate the necessity for the constrained version of the method, in Figure 2 we have applied the unconstrained method

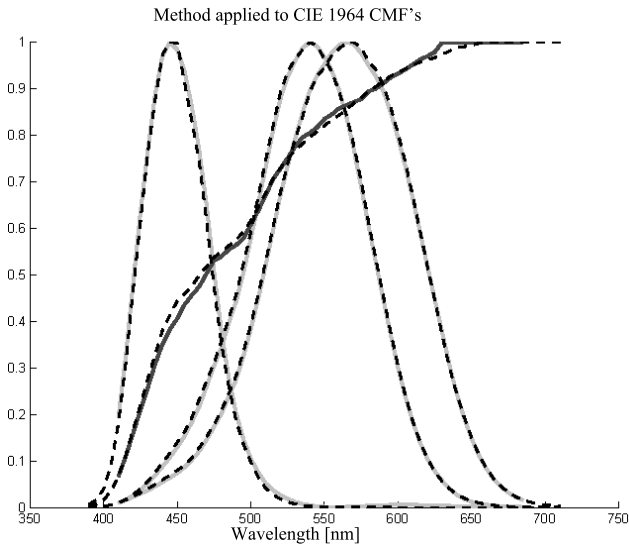


Fig. 7. The tabulated 10 degree cone fundamentals of the Stockman and Sharpe Sensor (black broken curves) and pre-filter (black broken curve) plotted with the estimated cone fundamentals in light gray full curves and the corresponding pre-filter in dark gray full curve. Results based on the constrained iterative method applied to the CIE1964 10 degree Standard Observer Color Matching Functions.

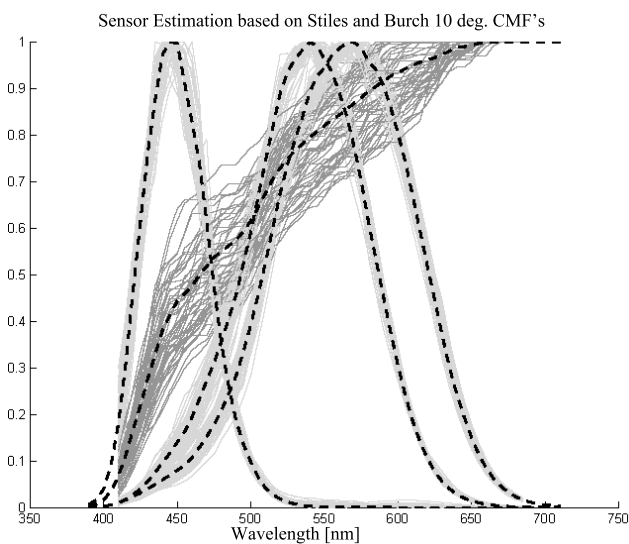


Fig. 8. Sensor estimation based on individual Stiles-Burch 10 deg. (1959) color matching functions. The constrained iterative method. Estimated fundamentals alternatively calculated by pre-filters absorbances (light gray full curves), Estimated pre-filters (dark gray full curves), Stockman and Sharpe cone fundamentals (black broken curves) and pre-filter (black broken curves)

to the Stiles and Burch 10 degree color matching functions and plotted the estimated cone functions. Slight negative lobes of the S cone estimations are present along with some ringing (departures from monotonicity) especially in the long wavelength part of the pre-filter estimations. To contain these phenomena we implement the constrained approach. The results of applying the constrained method to the 51 individual Stiles and Burch 10 degree color matching functions are shown in Figure 8.

In Figure 9 the results corresponding to the application of the method to the Stiles and Burch 2 degree color matching functions are also shown. The darker gray full curves are the estimations of each pre-filter pertaining to each set of cone fundamental estimations shown in light gray full curves. The black broken curves are the Stockman and Sharpe pre-filters and the corresponding cone fundamentals for each set of color matching functions. In both cases the cone fundamental estimations are seen to be positive and the pre-filter estimations are monotonically non-decreasing.

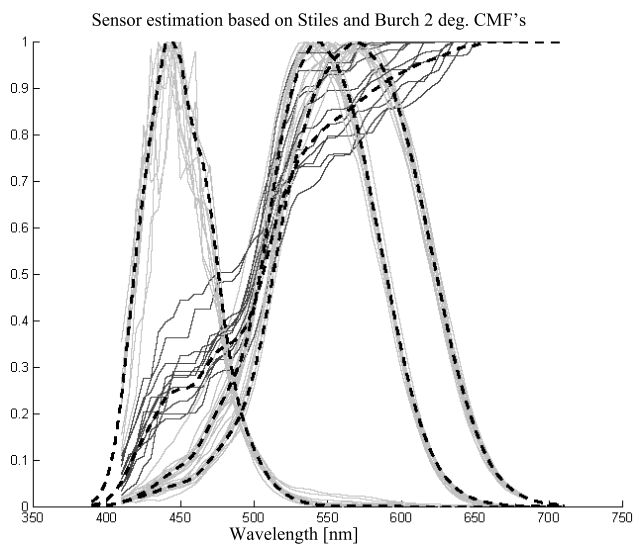


Fig. 9. Sensor estimation based on individual Stiles-Burch 2 deg. (1955) color matching functions. The constrained iterative method. Estimated fundamentals, (light gray full curves), Estimated pre-filters (dark gray full curves), Stockman and Sharpe cone fundamentals (black broken curves) and pre-filter (black broken curves)

In Figure 10 we have plotted the estimations of the cone fundamentals and the pre-filters for the repeated experiment of R. N. Wilson with color matching functions shown in Figure 11.

Noting that, in the repeated experiments the absorbance functions underlying the color matching functions must be the same, it can be seen that the differences between the repeated color matching functions are mainly absorbed in the pre-filter estimations, thus leaving a rather stable cone fundamental estimation. This indicates that intra-individual differences may affect the cone fundamental estimation relatively little. Ideally the cone fundamental estimation would be unaffected by the intra-individual differences in the color matching functions, leading to the same set of functions. However, in the absence of any mechanism for removing noise from individual CMFs, these differences are necessarily propagated to either or both of the pre-filter estimation or the matrix coefficients. The experimental observation that in our approach the noise is largely absorbed

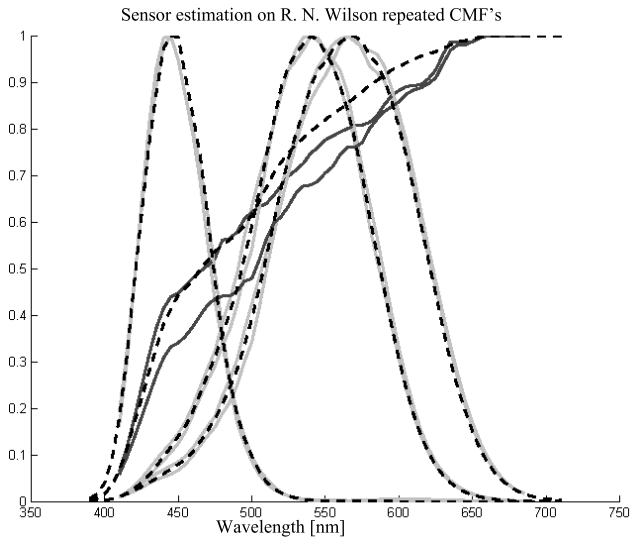


Fig. 10. Estimated cone fundamentals based on the constrained method, used on the repeated color matching function of R. N. Wilson (1959).

by the pre-filter is an interesting and non-intuitive property and warrants further discussion.

D. Related Predictions

To get a qualitative insight into how error represented by the difference between the assumed absorbance functions and the unknown real absorbance function for a specific individual may be propagating to the estimation of the matrix \mathbf{M} and the prefilter \mathbf{D} we can insert error variables into Equation 18:

$$[\mathbf{D} + \epsilon_D][\mathbf{W}_{cmf}][\mathbf{M} + \epsilon_M] = [\mathbf{W}_{pdt} + \epsilon_{pdt}] + \epsilon \quad (35)$$

where ϵ_D is a $N \times N$ diagonal matrix containing error propagated to the prefilter \mathbf{D} , ϵ_M is a 3×3 matrix containing the error propagated to the conversion matrix \mathbf{M} , ϵ_{pdt} is a $N \times 3$ matrix containing error originating from the incorrectly assumed absorbance functions \mathbf{W}_{pdt} and ϵ is an $N \times 3$ matrix allowing for optimization error, due to noise in the color matching functions, when Equation 19 is minimized. Setting $\epsilon_M \approx 0$ in Equation 35 then:

$$[\mathbf{D} + \epsilon_D]\mathbf{W}_{cmf}\mathbf{M} = \mathbf{W}_{pdt} + \epsilon_{pdt} + \epsilon \quad (36)$$

using Equation 18 in Equation 36:

$$\epsilon_D\mathbf{W}_{cmf}\mathbf{M} = \epsilon_{pdt} + \epsilon \quad (37)$$

and again in Equation 37 so that:

$$\epsilon_D\mathbf{D}^{-1}\mathbf{W}_{pdt} = \epsilon_{pdt} + \epsilon \quad (38)$$

Assuming that ϵ is uncorrelated with ϵ_{pdt} and that $\epsilon \ll \epsilon_{pdt}$ Equation 38 says that a modified prefilter $\epsilon_D\mathbf{D}^{-1}$ times the absorbance functions \mathbf{W}_{pdt} should be equal to the absorbance error functions. On a per function basis, this is feasible in the short wavelengths where the short wavelength absorbance function $t(\lambda)$ is active and the middle- and longwave absorbance functions are close to zero. Beyond the short wavelengths where the middle- and longwave absorbance functions are dominant and the shortwave absorbance is waning towards zero, the modified

prefilter will still be able to make the equation hold in bands of wavelengths where either of the corresponding absorbance error functions are approximately zero or locally equal.

If $\epsilon_D \approx 0$ then Equation 35 becomes:

$$\mathbf{D}\mathbf{W}_{cmf}\mathbf{M} + \mathbf{D}\mathbf{W}_{cmf}\epsilon_M = [\mathbf{W}_{pdt} + \epsilon_{pdt}] + \epsilon \quad (39)$$

again using Equation 18:

$$\mathbf{D}\mathbf{W}_{cmf}\epsilon_M = \epsilon_{pdt} + \epsilon \quad (40)$$

and again in Equation 40 so that:

$$\mathbf{W}_{pdt}\mathbf{M}^{-1}\epsilon_M = \epsilon_{pdt} + \epsilon \quad (41)$$

Equation 41 says that the absorbance functions should be linearly related to the absorbance error functions ϵ_{pdt} by a modified conversion matrix $\mathbf{M}^{-1}\epsilon_M$. This can clearly not be the case since that linear relation would imply the existence of more than one solution to Equation 18 which is disproved by Equations 27 to 31.

Bearing in mind that there is only one unique solution to Equation 18 then it is quite feasible that most of the error in the absorbance functions is compensated in the estimated prefilter function. This means, discounting the noise in the color matching functions, that the conversion matrix is quite close to the matrix that indeed would relate the individual color matching functions to their real individual fundamentals.

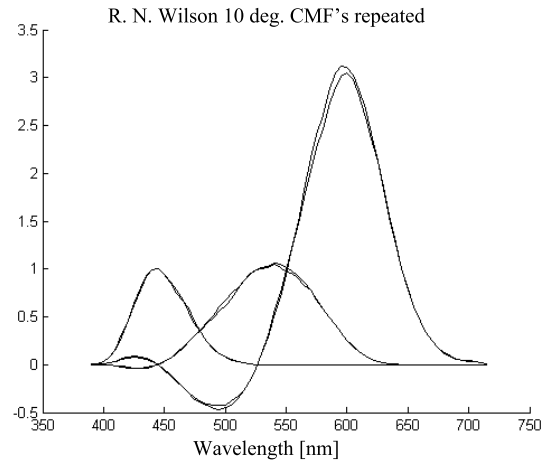


Fig. 11. Plot of two color-matching-functions sets measured for a single observer, R.N.Wilson. Results are derived from two identical experiments, and differences correspond to noise in the measurement process.

5. CONCLUSION

We have presented a novel method to estimate individual cone fundamentals based on the corresponding color matching functions. The method simultaneously estimates a pre-filter that constitutes the combined macular and ocular pre-filtration. The method is iterative and based on linear optimization and it relies on the assumption that the photo-pigment spectral absorbances pertaining to the individual color matching functions are known a priori.

We have applied the method on two sets of individual Stiles and Burch color matching functions, pertaining to the 2 and

10 degree viewing fields. The results show that the proposed method gives cone fundamentals that are remarkably similar to the corresponding functions derived by Stockman and Sharpe from the Stiles and Burch data, even though we use a more general constraint, that does not take into account variation in peak optical densities and peak wavelengths. Thus, we expect that some variation between the true individual cone fundamentals and the estimated is present in the results. Especially the overlap between the middle- and long- wavelength cones can cause such variation. The method demonstrates robustness towards intra-individual differences in color matching functions, which would be expected from a method that indeed leads to the correct estimations. While we have no objective measure for the quality of these estimates, the performance of the method on the Stiles and Burch 2- and 10-degree color matching functions suggests by visual inspection of the results and through the error propagation analysis, that the estimations will be close to the true fundamentals.

6. APPENDIX

A. Convergence optimisation

In our experiments we also employ a technique for enhancing the speed of convergence. We do this by reducing the number of linear least squares equations from N to one. Equation 19 is reformulated with regard to \mathbf{D} by projecting onto the orthogonal complement [31] to the subspace of \mathbf{R}^N spanned by \mathbf{W}_{pdt} . So instead of finding a pre-filter \mathbf{D} , that minimizes the distance between $\mathbf{D}\mathbf{W}_{cmf}\mathbf{M}$ and \mathbf{W}_{pdt} by N optimizations, as expressed by Equation 20, we minimize the projection of $\mathbf{D}\mathbf{W}_{cmf}\mathbf{M}$ onto the orthogonal complement of \mathbf{W}_{pdt} in which case only one optimization is necessary. In our Matlab implementation this reduces the convergence time to about one 15th.

The $N \times N$ dimensional projection matrix \mathbf{P} for the orthogonal complement of a subspace of \mathbf{R}^N spanned by the 3 column vectors of the $N \times 3$ dimensional matrix \mathbf{W}_{pdt} is given [32] by:

$$\mathbf{P} = \mathbf{I} - \mathbf{W}_{pdt}(\mathbf{W}_{pdt}^T \mathbf{W}_{pdt})^{-1} \mathbf{W}_{pdt}^T \quad (42)$$

where \mathbf{I} is an $N \times N$ dimensional identity matrix. Since $\mathbf{W}_{lms} = \mathbf{W}_{cmf}\mathbf{M}$ (Equation 3) then, by applying \mathbf{P} on both sides of Equation 18 and subsequently rearranging so \mathbf{D} becomes an $N \times 1$ vector \mathbf{d} , Equation 20 can be replaced by:

$$\min_{\mathbf{d}} \|\mathbf{P}^* \mathbf{W}_{lms}^k \mathbf{d} - \mathbf{0}^*\|^2 \quad (43)$$

where \mathbf{P}^* is a $3N \times 3N$ dimensional projection matrix, containing zeros except three repetitions of matrix \mathbf{P} along the diagonal, \mathbf{W}_{lms}^k is a $3N \times N$ block diagonal matrix containing zeros except in each of its three consecutive diagonals, being occupied by each of the three columns from matrix \mathbf{W}_{lms} , $\mathbf{0}^*$ is a $3N \times 1$ dimensional zero-vector and for vector \mathbf{d} applies $\mathbf{d}_i = \mathbf{D}_{ii}^{k+1}$. In order to avoid the obvious solution $\mathbf{d}_i = 0$ for $i = 1..N$ an additional constraint on the pre-filter function is employed:

$$\sum_{i=1}^N d_i = 1 \quad (44)$$

Equation 44 simply ensures that the pre-filter estimate is a function that integrates to a unit area. The linear scale of the pre-filter function is countered by the scale of the coefficients in \mathbf{M} and will thus have no influence on the solution. In matrix terms Equation 44 translates to:

$$\mathbf{A}_{eq} \mathbf{d} = 1 \quad (45)$$

where \mathbf{A}_{eq} is a $1 \times N$ dimensional vector containing ones. Equations 43, 24 and 45 together form a quadratic programming problem to solve for \mathbf{d} and thereby \mathbf{D}^{k+1} .

7. ACKNOWLEDGEMENTS

The authors would like to thank Professor Ivar Farup, IMT, NTNU in Gøvik, Norway for his valuable comments.

REFERENCES

1. Commission Internationale d'Eclairage, "Downloads," <http://www.cie.co.at>, Last Accessed July 2015.
2. G. Wyszecki, and W. S. Stiles, "Color Science," Wiley, New York, (1982).
3. Mark D. Fairchild, *Color Appearance Models*, (3rd Ed. Wiley-IS&T, Chichester, UK, 2013.)
4. H. J. A. Dartnall, J. K. Bowmaker and J. D. Mollon, "Human visual pigments, microspectrophotometric results from the eyes of seven persons," *Proceedings of the Royal Society of London* **220**, Vol. B, 115–130 (1983).
5. J. L. Schnapf, T. W. Kraft and D. A. Baylor, "Spectral sensitivity of human cone photoreceptors," *Nature* **325**, 439–441 (1987).
6. A. Stockman and L. T. Sharpe, "The spectral sensitivities of the middle- and long-wavelength-sensitive cones derived from measurements in observers of known genotype," *Vision Research* **40**, Number 13, 1711–1737 (2000).
7. J. Neitz, and G. H. Jacobs, "Polymorphism in normal human color vision and its mechanism," *Vision Research* **30**, Number 4, 621–36 (1990)
8. S. L. Merbs and J. Nathans, "Absorption Spectra of Human Cone Pigments," *Nature* **356**, 433–435 (1992).
9. J. Pokorny, VC Smith, G. Verriest and A. Pinckers, "Congenital and Acquired Color Vision Defects," New York: Grune and Stratton (1979).
10. M. M. Bongard and M. S. Smirnov, "Determination of the eye spectral sensitivity curves from spectral mixture curves," *Dokl Akad Nauk SSSR* **102**, Number 6, 1111–1114 (1954).
11. C. F. Andersen, "Simplified cone fundamental estimation," in *New results in color characterization of humans and cameras*, (Academic, 2010), 58–84.
12. C. F. Andersen and G. D. Finlayson, "Estimation of an individuals human cone fundamentals from their color matching functions," in *Proceedings Color in Graphics Imaging and Vision (CGIV)* (2010).
13. D. A. Macleod and M. A. Webster, "Factors underlying individual differences in the color matches of normal observers," *Journal of Optical Society of America A* **5**, Number 10, (1988).
14. A. Knowles and H. J. A. Dartnall, "The photobiology of vision," in *The Eye*, Vol. 2B H. Davson, ed. (London/New York: Academic, 1997), p.77. (1997).
15. J. J. Vos and P. L. Walraven, "On derivation of the foveal receptor primaries," *Vision Research* **11**, Number 8, 799–818 (1971).
16. A. Stockman, L. T. Sharpe and C. C. Fach, "The spectral sensitivities of the human short-wavelength cones," *Vision Research* **39** 2901–2927 (1999).
17. V. C. Smith and J. Pokorny, "Spectral sensitivity of the foveal cone photo-pigments between 400 and 500 nm," *Vision Research* **15**, Number 2, 161–171 (1975).
18. N. I. Speranskaya and N. V. Lobanova, "Determination of the spectral sensitivity curves of the optical receptors of anomalous trichromats," *Biophysics* **6**, Number 5, 596–604 (1961).
19. N. I. Speranskaya and N. V. Lobanova, "Determination of the spectral sensitivity curves of the optical receptors of normal trichromats," *Biophysics* **6**, Number 4, 596–604 (1961).
20. A. D. Logvinenko, "On derivation of spectral sensitivities of the human cones from trichromatic color matching functions," *Vision Research* **38**, 3207–3211 (1998).
21. J. D. Mollon, "Color Vision, Opsins and Options,". *Proceedings of the National Academy of Sciences of the United States of America* **96**, Number 9, 4743–4745 (1999).
22. T. D. Lamb, "Photoreceptor Spectral Sensitivities: Common Shape in the Long-wavelength Region," *Vision Research* **35**, Number 35, 3083–3091 (1995).

23. D. G. Stavenga, R. P. Smits and B. J. Hoenders, "Simple Exponential Functions Describing the Absorbance Bands of Visual Pigment Spectra," *Vision Research* **33**, Number 8, 1011–1007 (1993).
24. D. A. Macleod and Michael A. Webster, "Direct psychophysical estimates of the cone-pigment absorption spectra," *Journal of Optical Society of America A* **5**, Number 10, (1988).
25. CIE, TC136, "Fundamental chromaticity diagram with physiological axes," CIE technical report, **CIE 170-1** (2006).
26. J. M. Palmer, *Handbook of Optics*, Palmer, J. M. (1995). *The measurement of transmission, absorption, emission, and reflection*. In *Handbook of Optics II* (ed. M. Bass, E. W. Van Strylan, D. R. Williams and W. L. Wolfe), pp. 25.1-25.25. New York: McGraw-Hill Inc.
27. "Photopigments," <http://www.cvrl.org>, Last accessed June 15, 2016
28. D. G. Stavenga, "On visual pigment templates and the spectral shape of invertebrate rhodopsins and metarhodopsins," in *Journal of Comparative physiology A*, (Springer), 869–878 (2010).
29. V. I. Govardovskii, N. Fyhrquist, T. Reuter, D.G. Kuzmin and K. Donner, "In search of the visual pigment template," in *Visual Neuroscience* **17**, 509–528 (2000).
30. Y. Asano, M. D. Fairchild, L. Blondé, "Development of a vision model for individual colorimetric observers," OSA fall vision meeting, Philadelphia, PA, 2014.
31. G. Strang, *Linear Algebra and its applications*, (Harcourt Brace Jovanovich College Publishers, 1986), p.138.
32. G. Strang, *Linear Algebra and its applications*, (Harcourt Brace Jovanovich College Publishers, 1986), p.156.
33. A. Stockman and L. T. Sharpe, "Spectral sensitivities and color matching," in *Color Vision from genes to perception*, K. R. Gegenfurtner and L. T. Sharpe, eds. (Cambridge University Press: Academic, 1999), p.65. (1999).
34. W. S. Stiles and J. M. Burch, "Interim report to the Commission Internationale de l'Eclairage Zurich, on the National Physical Laboratory's investigation of color-matching (1955) with an appendix by W. S. Stiles and J. M. Burch," *Optica Acta* **2** 168–181 (1955).
35. W. S. Stiles and J. M. Burch, "NPL color-matching investigation: Final report," *Optica Acta* **6** 1–26 (1959).
36. P. W. Trezona, "Individual observer data for the 1955 Stiles-Burch 2 degree pilot investigation," *Journal of Optical Society of America A* **4**, Number 4, 769–782 (1987).
37. A. D. Logvinenko, "On the colors dichromats see," *Color Res. Appl.* **38**, Number 4, (2012).